Palladium complexes containing NNN pincer type ligands and their activities in Suzuki-Miyaura cross coupling reaction

Ebru Keskin, Hakan Arslan[*]

Department of Chemistry, Faculty of Science, Mersin University, Mersin, TR33343, Türkiye

ARTICLE INFO

ABSTRACT

Five new NNN pincer-type ligands and their palladium complexes were successfully synthesised and characterised by FT-IR, ^{1}H NMR, ^{13}C NMR, and UV–vis analyses. TEM analysis was used to observe the morphological character of the black residues obtained from the fourth cycle of the reusability test. Furthermore, suitable crystals of the N^2,N^6-*bis*(2-*tert*-butylphenyl)pyridine-2,6-dicarboxamide and its palladium complex were elucidated with the X-ray single crystal diffraction method. Both the ligand and its palladium complex crystallise in a monoclinic system with space group $P2_1/c$ for the H_2L^4 and $C2/c$ for the palladium complex. The structure of the pincer ligand and its palladium complex were stabilised by intramolecular and intermolecular C–H⋯O, C–H⋯N, and N–H⋯N contacts. A Suzuki-Miyaura cross-coupling reaction between aryl halides and phenylboronic acid was used to assess the catalytic abilities of the palladium pincer complexes. All of the prepared complexes exhibited considerable catalytic activity. However, complexes 4 (Acetonitrile-N^2,N^6-bis(2-*tert*-butylphenyl)pyridine-2,6-dicarboxamidopalladium(II)) and 5 (Acetonitrile-N^2,N^6-bis(2-nitrophenyl)pyridine-2,6-dicarboxamidopalladium(II)) provided almost 100% conversion with nearly 100% yield in the reaction between 4-bromotoluene and phenylboronic acid. Furthermore, these active complexes catalysed the reaction of the sterically hindered and deactivated substrates (1-Bromo-4-izobutylbenzene and 2-bromo-6-methoxynaphthalene) with phenylboronic acid, and complete conversion and yields up to 100% were achieved in a short time with the 2-bromo-6-methoxynaphthalene.

1. Introduction

Some of the versatile organometallic catalysts utilized in organic synthesis for the production of carbon-carbon and carbon-heteroatom bonds include organopalladium compounds. An ideal organometallic catalyst should have strong catalytic activity even at low catalyst loadings, together with stability and selectivity [1]. Carbon-carbon bond formation reactions are among the important reactions in chemistry as they provide key steps in the construction of complex bioactive molecules, such as pharmaceuticals and agrochemicals. These reactions are also essential in the development of innovative organic materials with new electronic, optical, or mechanical effects that probably play an important role in the evolving branches of nanotechnology [2]. Over the past 40 years, the most important methodologies for the formation of carbon-carbon bonds have involved the use of transition metals to mediate reactions in a controlled and selective manner. C–C cross-coupling reactions are described as carbon-carbon bond reactions that occur between an organic electrophile and an organometallic nucleophile in the presence of a metal catalyst. The catalysts used in these

---

reactions are generally transition-metal complexes, especially nickel and palladium metals. These two metals are involved in the wide majority of cross-coupling reactions, because of the ease of interchange of redox steps, that is, conversions such as Ni(+2)/Ni(0) and Pd (+2)/Pd(0), which is a basic necessity to complete the catalytic cycle [3]. The Pd(0)/Pd(II) catalytic cycles are prone to the inherent drawbacks of β-hydride elimination from Pd (II), often resulting in irreversible rupture of the palladium-carbon bond and subsequent decomposition of the complex. Various research groups have reported that, in many instances, the true catalysts involved in C–C bond coupling utilising palladacycles are not necessarily the palladacycles or pincer palladium complexes themselves, but rather palladium nanoparticles or other weakly low-ligated palladium species. However, Milstein and his colleagues demonstrated that under mild reaction conditions, the palladium(II) center in pincer complexes can undergo reversible Pd(II) to Pd(IV) transformations, as evidenced by their study [4]. In contrast to the Pd(0)/Pd(II) cycle, the Pd(II)/Pd(IV) cycle offers greater promise for the facile reductive elimination step from a Pd(IV) center and exhibits enhanced chemoselectivity for the oxidative addition on Pd(II). However, the oxidation of Pd(II) to Pd(IV) poses a thermodynamically unfavourable process as a result of the electronic deficiency of the Pd(IV) center. In this context, taking into account the strong electron-donating nature of pincer ligands, they appear to be a suitable choice for supporting and stabilising Pd(IV) complexes. Until now, numerous studies have reported Pd(IV) pincer complexes as catalytic intermediates, thus broadening the application range of palladium-based catalysts [5–8].

Since the first work on palladium pincer complex catalysts was published by Milstein and coworkers as part of the Heck reaction, numerous studies on cross-linking reactions have been published. The most extensive studies in this field are Heck-coupling/Heck-type reactions and Suzuki-Miyaura cross-coupling reactions [9]. Usually homogeneous catalytic systems previously reported are phosphine ligand-based systems. Though the catalytic activity of transition metal complexes with phosphine ligands is well, the sensibility of ligands and complexes to air makes them less attractive [10–12]. The electronic and structural properties of the metal center used in catalysis can be improved by the appropriate selection of the chelating arms of the pincer ligand [13]. The notable stability achieved by employing tridentate ligands is a fundamental characteristic of pincer complexes, allowing their use as catalysts under high-temperature conditions [14]. Palladium(II) complexes based on the NNN pincer type ligand have become very remarkable due to their favourable balance between stability and reactivity and their high catalytic activity in C–C bond formation reactions [15–18]. Furthermore, many of these complexes are stable to air and moisture, making them easy to transport and store, providing long-lasting catalysts and broad reaction coverage [9]. In view of these studies, the aim of our study is to investigate the new types of pincer complexes and their catalytic roles in the Suzuki-Miyaura cross-coupling reaction. For this purpose, we synthesised five new pincer-type pyridine-2,6-dicarboxamide NNN ligands and their palladium complexes and characterised by various methods. Furthermore, the catalytic activities of the palladium complexes were tested in the Suzuki-Miyaura cross-coupling reaction.

2. Experimental

2.1. Instrumentations

The synthesised compounds were subjected to various analytical techniques to elucidate their properties. ^{1}H and ^{13}C NMR analysis was carried out using a Bruker UPB Avance-III 400 MHz NMR spectrometer. TMS was used as an internal standard in dimethyl sulfoxide-d_6 on the scale in ppm. The pincer ligands were analyzed using FT-IR spectroscopy with a PerkinElmer Frontier Spectrum100 ATR spectrometer. Using a Shimadzu GC-2030 instrument with a 30 m × 0.25 mm RTX-5 capillary column and FID detector, the catalytic activity of Pd complexes in the C–C cross coupling process was assessed. UV–vis spectroscopy was employed to examine the spectra of the pincer ligands and their palladium complexes on a Shimadzu UV-3100 spectrometer. With Cu-Kα radiation, X-ray single-crystal analysis (SCXRD) was performed using a Bruker CCD APEX-II diffractometer. The crystals were kept at room temperature throughout the analysis, and the solution was achieved using the OLEX2 [19] program, the Superflip [20–22] structure resolution program, the Charge Flipping resolution technique, and the full matrix least squares method on F^2 by ShelXL [23], with the refinement of F^2 against all reflections. Hydrogen atoms were refined isotropically, and all non-H atoms were refined anisotropically, while the refinement of the molecule's molecular structure graphics was created with OLEX2 program [19].

2.2. Synthesis of pyridine-2,6-dicarboxamide NNN pincer ligands

2.2.1. Synthesis method for H₂L¹⁻³

All experimental process were carried out in open atmosphere. First, the precursor compound pyridine-2,6-dicarbonylchloride was synthesised from pyridine-2,6-dicarboxylic acid (the synthesis details and characterization data were given in supplementary material)
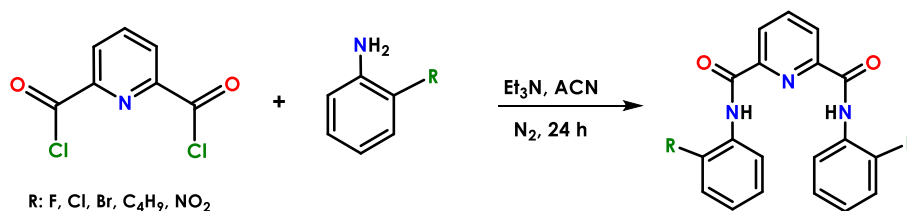
Scheme 1. Synthesis of H₂L¹⁻⁵ ligands.

[24]. Et$_3$N (10 mmol, 1.01 g) and related aniline derivatives (2-fluoroaniline, 2-chloroaniline, and 2-bromoaniline, 10 mmol) were added to the solution of the compound of pyridine-2,6-dicarbonylchloride (5 mmol) in acetonitrile (50 mL), under N$_2$ atmosphere, respectively. The mixture was stirred at room temperature for 24 h. The precipitated solid was filtered off, washed with ether two times, and dried in vacuo (Scheme 1).

N^2,N^6-bis(2-Fluorophenyl)pyridine-2,6-dicarboxamide (**H$_2$L^1**): Color: White. Yield: 77%. ^{1}H NMR (400 MHz, DMSO-d_6): δ 10.93 (s, 2H, NH), 8.40 (t, 2H, H$_{Ar}$), 8.36–8.32 (m, 1H, H$_{Ar}$), 7.72 (t, 2H, H$_{Ar}$), 7.39 (t, 4H, H$_{Ar}$), 7.34–7.31 (m, 2H, H$_{Ar}$) ppm. ^{13}C NMR (100 MHz, DMSO-d_6): δ 161.97 (C=O), 155.37, 154.92, 148.27, 140.15, 125.39, 124.92, 124.54 (C$_{Ar}$) ppm. FTIR (ν, cm^{-1}): 3360, 3272 (N–H), 3091 (Ar–H), 1672 (C=O).

N^2,N^6-bis(2-Chlorophenyl)pyridine-2,6-dicarboxamide (**H$_2$L^2**): Color: White. Yield: 80%. ^{1}H NMR (400 MHz, DMSO-d_6): δ 10.90 (s, 2H, NH), 8.42 (t, 2H, H$_{Ar}$), 8.37–8.33 (m, 1H, H$_{Ar}$), 7.80 (d, 2H, H$_{Ar}$), 7.65 (dd, 2H, H$_{Ar}$), 7.48 (td, 2H, H$_{Ar}$), 7.38 (td, 2H, H$_{Ar}$) ppm. ^{13}C NMR (100 MHz, DMSO-d_6): δ 161.81 (C=O), 148.60, 140.26, 134.18, 127.74, 124.06 (C$_{Ar}$) ppm. FTIR (ν, cm^{-1}): 3363, 3270 (N–H), 3110 (ArH), 1673 (C=O).

N^2,N^6-bis(2-Bromophenyl)pyridine-2,6-dicarboxamide (**H$_2$L^3**): Color: White. Yield: 75%. ^{1}H NMR (400 MHz, DMSO-d_6): δ 10.93 (s, 2H, NH), 8.41 (t, 2H, H$_{Ar}$), 8.34–8.30 (m, 1H, H$_{Ar}$), 7.78 (dd, 2H, H$_{Ar}$), 7.69 (dd, 2H, H$_{Ar}$), 7.50 (td, 2H, H$_{Ar}$), 7.29 (td, 2H, H$_{Ar}$) ppm. ^{13}C NMR (100 MHz, DMSO-d_6): δ 161.83 (C=O), 148.36, 140.25, 132.78, 128.30, 125.39 (C$_{Ar}$) ppm. FTIR (ν, cm^{-1}): 3343, 3263 (N–H), 3113 (ArH), 1673 (C=O).

2.2.2. Synthesis method for H$_2$L^{4,5}

The solution of aniline (2-*tert*-butylaniline, 2-nitroaniline, 10 mmol) and Et$_3$N (10 mmol) in acetonitrile (10 mL) was kept in an ice bath for 2 h and added dropwise for 3 h over the solution of compound pyridine-2,6 dicarbonylchloride (5 mmol) in acetonitrile (50 mL). The solution was stirred under N$_2$ atmosphere. At the end of the reaction, which lasted for 24 h under room conditions, the solution was evaporated. The resulting white solid product was washed with ether and dried in vacuo (Scheme 1).

N^2,N^6-bis(2-tert-Butylphenyl)pyridine-2,6-dicarboxamide (**H$_2$L^4**): Color: White. Yield: 80%. ^{1}H NMR (400 MHz, DMSO-d_6): δ 10.87 (s, 2H, NH), 8.39 (t, 2H, H$_{Ar}$), 8.33–8.29 (m, 1H, H$_{Ar}$), 7.52 (dd, 2H, H$_{Ar}$), 7.36–7.29 (m, 4H, H$_{Ar}$), 7.17 (dd, 2H, H$_{Ar}$), 1.36 (s, 18H, H$_{CH3}$) ppm. ^{13}C NMR (100 MHz, DMSO-d_6): δ 162.76 (C=O), 148.97, 147.44, 139.91, 135.77, 131.74, 124.81 (C$_{Ar}$), 34.96 (C$_{CH3}$), 31.02 (CH$_3$) ppm. FTIR (ν, cm^{-1}): 3341 (N–H), 3078 (ArH), 1671 (C=O).

N^2,N^6-bis(2-Nitrophenyl)pyridine-2,6-dicarboxamide (**H$_2$L^5**): Color: Yellow. Yield: 84%. ^{1}H NMR (400 MHz, DMSO-d_6): δ 11.75 (s, 2H, NH), 8.44–8.36 (m, 3H, H$_{Ar}$), 8.20 (t, 4H, H$_{Ar}$), 7.88 (t, 2H, H$_{Ar}$), 7.50 (t, 2H, H$_{Ar}$) ppm. ^{13}C NMR (100 MHz, DMSO-d_6): δ 161.66 (C=O), 147.85, 141.30, 134.91, 125.95, 124.94 (C$_{Ar}$) ppm. FTIR (ν, cm^{-1}): 3372, 3329 (N–H), 3094 (ArH), 1666 (C=O).

### 2.3. General method for the synthesis of NNN palladium(II) pincer complexes (1–5)

Palladium(II) acetate salt (1.2 mmol) dissolved in hot acetonitrile was added dropwise to the solution of the ligand (1 mmol) in hot acetonitrile under reflux. When the reaction colour changed from red to yellow, the temperature was reduced and the reaction was stirred at room temperature for one week. At the end of this period, the solution was evaporated and the oily product obtained was crystallized from acetonitrile and diethyl ether mixture (Scheme 2).

Acetonitrile-N^2,N^6-bis(2-fluorophenyl)pyridine-2,6-dicarboxamidopalladium(II) (**1**): Color: Yellow. Yield: 80%. ^{1}H NMR (400 MHz, DMSO-d_6): δ 8.34 (t, 1H, H$_{Ar}$), 7.83 (d, 2H, H$_{Ar}$), 7.26–7.12 (m, 8H, H$_{Ar}$), 2.07 (s, 3H, CH$_3$CN) ppm. ^{13}C NMR (100 MHz, DMSO-d_6): δ 166.55 (C=O), 157.12 (C$_{CN}$), 154.68, 150.16, 141.09, 132.84, 128.30, 122.85, 114.55 (C$_{Ar}$), 1.14 (C$_{CH3}$) ppm.

Acetonitrile-N^2,N^6-bis(2-chlorophenyl)pyridine-2,6-dicarboxamidopalladium(II) (**2**): Color: Yellow. Yield: 75%. ^{1}H NMR (400 MHz, DMSO-d_6): δ 8.35 (t, 1H, H$_{Ar}$), 7.84 (d, 2H, H$_{Ar}$), 7.45 (d, 2H, H$_{Ar}$), 7.28 (t, 4H, H$_{Ar}$), 7.22–7.18 (m, 2H, H$_{Ar}$), 2.07 (s, 3H, CH$_3$CN) ppm. ^{13}C NMR (100 MHz, DMSO-d_6): δ 166.10 (C=O), 150.27 (C$_{CN}$), 142.79, 141.10, 129.72, 128.39, 128.12, 126.13, 125.24, 124.67 (C$_{Ar}$), 1.13 (C$_{CH3}$) ppm.

Acetonitrile-N^2,N^6-bis(2-bromophenyl)pyridine-2,6-dicarboxamidopalladium(II) (**3**): Color: Yellow. Yield: 84%. ^{1}H NMR (400 MHz, DMSO-d_6): δ 8.34 (t, 1H, H$_{Ar}$), 7.85 (d, 2H, H$_{Ar}$), 7.62 (dd, 2H, H$_{Ar}$), 7.35–7.29 (m, 4H, H$_{Ar}$), 7.12 (td, 2H, H$_{Ar}$). 2.07 (s, 3H, CH$_3$CN) ppm. ^{13}C NMR (100 MHz, DMSO-d_6): δ 166.81 (C=O), 151.23 (C$_{CN}$), 145.47, 129.41, 127.77, 125.89, 121.78 (C$_{Ar}$), 1.12 (C$_{CH3}$) ppm.

Acetonitrile-N^2,N^6-bis(2-tert-butylphenyl)pyridine-2,6-dicarboxamidopalladium(II) (**4**): Color: Yellow. Yield: 78%. ^{1}H NMR (400 MHz, DMSO-d_6): δ 8.33 (t, 1H, H$_{Ar}$), 7.80 (d, 2H, H$_{Ar}$), 7.36 (dd, 2H, H$_{Ar}$), 7.19 (dd, 1H, H$_{Ar}$), 7.15 (dd, 2H, H$_{Ar}$), 7.12 (td, 3H, H$_{Ar}$), 2.10 (s, 3H, CH$_3$CN), 1.51 (s, 18H, H$_{CH3}$) ppm. ^{13}C NMR (100 MHz, DMSO-d_6): δ 167.67 (C=O), 152.35 (C$_{CN}$), 146.70, 145.66, 141.77, 130.28,
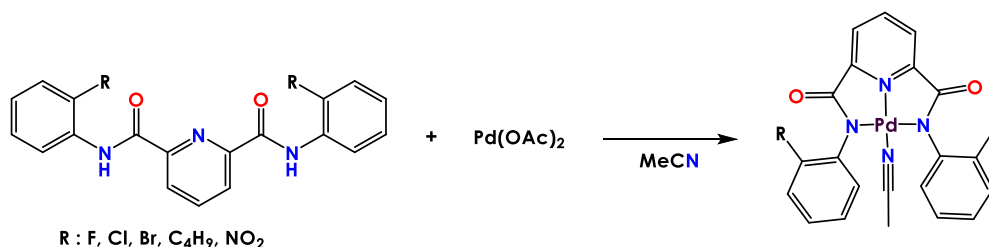
Scheme 2. Synthesis of NNN palladium(II) pincer complexes.

126.98, 126,48, 125.21, 125.10 (C_{Ar}), 35.53 (C_{CH3}), 31.43 (CH_3), 1.12 (C_{CH3}) ppm.

Acetonitrile-N^2,N^6-bis(2-nitrophenyl)pyridine-2,6-dicarboxamidopalladium(II) (**5**): Color: Yellow. Yield: 82%. ^{1}H NMR (400 MHz, DMSO-d_6): δ 8.40 (t, 1H, H_{Ar}), 7.91 (t, 4H, H_{Ar}), 7.69 (td, 2H, H_{Ar}), 7.41 (td, 4H, H_{Ar}), 2.10 (s, 3H, CH_3CN) ppm. ^{13}C NMR (100 MHz, DMSO-d_6): δ 167.58 (C=O), 150.94 (C_{CN}), 145.52, 142.51, 133.14, 126.38, 125.41, 124.32 (C_{Ar}), 1.12 (C_{CH3}) ppm.

2.4. Suzuki-Miyaura cross-coupling reaction method

The reaction of phenylboronic acid (1.2 mmol), arylbromide (1.0 mmol), organic solvent (2 mL), base (1.2 mmol), and palladium catalyst (0.001 mmol) was carried out in a closed tube at 110 °C for the required duration. The resulting mixture was subsequently treated with brine and saturated ammonium chloride solution, and the organic phase was separated and dried using anhydrous Na_2SO_4. The dried mixture was then filtered and evaporated [25,26]. To isolate the product, the crude mixture was mixed with ethyl acetate (15 mL) and subjected to chromatography on silicagel. The resulting isolated product was then characterized using ^{1}H NMR and GC analysis, with dodecane added as an internal standard prior to the GC analysis.

3. Results and discussion

3.1. Synthesis

In the first step of the synthesis part of this study, new pyridine-2,6-dicarboxamide, NNN pincer-type ligands were synthesised and the synthesised compounds were characterised by ^{1}H NMR, ^{13}C NMR, COSY, HMQC and FT-IR techniques. In the second step of the synthesis, palladium (II) complexes of these NNN pincer-type ligands were synthesised by the method specified in the synthesis part and their structures were elucidated by ^{1}H NMR, ^{13}C NMR, and FT-IR methods. Characterisation data for all prepared compounds are in agreement with the values in the literature [27–29].

FTIR measurements of the synthesised ligands were performed in the range of 450–4000 cm^{-1}. When the frequencies of the functional groups in the structure of the ligands were examined, the stretching frequencies of the NH groups were recorded in the range of 3263–3372 cm^{-1} for the H_2L^{1-5} compounds [30,31]. The stretching vibrations detected at 1672, 1673, 1673, 1671, and 1666 cm^{-1} for the H_2L^{1-5} ligands, respectively, are assigned to the carbonyl ν(C=O) stretching vibration mode and these results are in agreement with previous studies [32–34]. In agreement with previous work [34], the IR frequencies of the ν(C_{Ar}-H) group in the structure of the compounds were monitored in the range of 3078–3113 cm^{-1}. The data obtained from the FTIR study are compatible with the literature [35–37] and these data confirmed the structure of the prepared NNN pincer type compounds.

In the ^{1}H NMR spectrum of pincer ligands, amide proton signals appeared at δ 10.93, 10.90, 10.93, 10.87, 11.75 ppm, respectively, for the H_2L^{1-5} compounds [38]. Due to the electronegative nature of the nitro group, the amide proton of the H_2L^5 compound was resonated in the lower field (δ 11.75 ppm). The protons of the pyridine ring, which are common in the structure of the compounds, resonate in common, except for the H_2L^5 compound, in the triplet form of two protons in the range of δ 8.37–8.29 ppm, and the remaining proton as a multiplet in specific intervals for each compound. In the compound H_2L^5, three protons in the pyridine ring were observed as multiplets in the range of δ 8.44–8.36 ppm. According to the data from the literature [39], other aromatic protons were found in the predicted range of δ 8.20–7.17 ppm. The methyl protons in the *tert*-butyl group in the H_2L^4 compound appeared as a singlet at δ 1.36 ppm. The signals from the carbonyl group were found in the ^{13}C NMR spectra at 161.97, 161.81, 161.83, 162.76 and 161.66 ppm for the H_2L^{1-5} compounds, respectively. The aromatic carbons in the structure of the ligands emerged between the range of δ 155.37–124.06 ppm. Although the quaternary carbon of the *tert*-butyl group in the H_2L^4 compound resonated at δ 34.96 ppm, the carbons of the methyl group were also observed at δ 31.02 ppm [40].

In the ^{1}H NMR spectra of the complexes, after complexation, the absence of resonance of the amide protons confirmed the co-ordination of amide nitrogen atoms with the Pd(II) ion after deprotonation [41]. In addition to this observation, the resonance values of the aromatic protons shifted as a consequence of coordination with the palldium (II) ion. In the ^{1}H NMR spectra of the palladium complex 4, the methyl protons shifted to a downfield (δ 1.51 ppm) different from the free ligand, due to electron withdrawal by the metal ion, leading to a decrease in the electron density [42]. The chemical shift value of CH_3CN methyl protons that have attached to palladium were detected at δ 2.07 and 2.10 ppm in the ^{1}H NMR spectra of the complexes [43]. In the ^{13}C NMR spectra of the complexes, carbons of the CN and CH_3 groups of acetonitrile coordinating with palladium were observed in the range of δ 150.27–157.12 and 1.12–1.14 ppm, respectively [44]. Carbonyl carbons of the palladium complexes were detected in the lower region between the δ 166.10–167.67 ppm different from the free ligands. The resonance values of the aromatic carbons shifted for each palladium complex after the complexation. In the ^{13}C NMR spectra of the palladium complex 4, the resonance values of the *tert*-butyl group shifted to downfield. As a result of this, the quaternary carbon of the ligand (δ 34.96 ppm) emerged at δ 35.53 ppm and the methyl carbon (δ 31.02 ppm) appeared at δ 31.43 ppm.

3.2. The analysis of molecular structure

The good quality block white crystals of the N^2,N^6-*bis*(2-*tert*-butylphenyl)pyridine-2,6-dicarboxamide (H_2L^4) ligand and the block yellow crystals of its NNN Pd pincer complex 4 were obtained in acetonitrile and the appropriate crystals were chosen for the X-ray single crystal analysis. H_2L^4 crystallized in the monoclinic space group $P2_1/c$ with $Z = 4$ while complex 4 generated in the monoclinic space group $C2/c$ with $Z = 8$. Detailed crystallographic data and structure refinement parameters for both H_2L^4 and complex 4 can be found in Table 1, and the molecular structure of the synthesised H_2L^4 ligand and its Pd complex 4 are depicted in Fig. 1a (H_2L^4) and 1b

(Complex 4).

In the crystal structure of the ligand, the carbonyl groups have a specific bond length for a double bond such as C1-02 1.213(4) and O1–C17 1.228(4) Å [45,46]. All C–N bonds in the structure are shorter than the average length of the C–N bond, which is 1.48 Å (Table 2) [27,45]. The angles, which are C12–N1–C16 118.4(2) and C17–N3–C18 124.0(3)° in the structure of the pincer ligand, which are close to 120°, show the sp^2 hybridization of the N1 and N3 atoms (Table 2).

The Pd complex was formed by the coordination of the Pd(II) ion with the pyridine nitrogen of the ligand and the nitrogen of the two amide groups in the ligand and the nitrogen of an acetonitrile compound. The sum of the angles around the Pd(II) metal center is 360°, which is indicating a square planar geometry (Table 2) [47]. Four-coordination of Pd has resulted in the formation of two five-membered chelate rings such as Pd1–N3–C1–C2–N1 and Pd1–N2–C7–C6–N1 (Fig. 1b). The chelate bite angles of these five-membered rings in complex 4 are N1–Pd1–N3 = 81.01(19) and N1–Pd1–N2 = 80.59(19)°. In addition, the bite angles of N (amide)-Pd-N$_{Acetonitrile}$ are found as N3–Pd1–N4 = 95.8(2) and N2–Pd1–N4 = 102.8(2)°. Furthermore, the angle of the N$_{Pyr-idine}$-Pd-N$_{Acetonitrile}$ bond was detected as N1–Pd1–N4 = 174.1(2)° (Table 2). The dihedral angle of N–C–C–N (Pd1–N1–C2–C1–N3 and Pd1–N1–C6–C7–N2) which contains amide nitrogen and pyridyl rings in the complex is 1.46°, demonstrates that the rings are almost coplanar [48]. Furthermore, the maximum deviation from the Pd1–N1–C2–C1–N3 plane was found to be 0.046 Å for the N3 atom, while it was determined to be 0.039 Å for the N2 atom in the Pd1–N1–C6–C7–N2 plane.

The length of the Pd-N$_{Acetonitrile}$ bond, which is Pd1–N4 = 2.022(5) Å in complex 4 is compatible with the length of the Pd-N$_{Acetonitrile}$ bond found in previous studies [44,49]. It was determined that the length of the carbonyl bond (C1–O1 = 1.243(7) Å) in the Pd complex was longer than that of the free ligand (C1–O2 = 1.213(4) Å) due to complexation. Some of the C–N bond lengths (C7–N2 = 1.354(7) and C2–N1 = 1.347(8) Å) of the Pd complex are longer than the corresponding bond lengths in the free ligand (C17–N3 = 1.348(4) and C12–N1 = 1.330(4) Å) as a consequence of coordination with the Pd metal (Table 2).

The crystal structure of the NNN pincer ligand and its Pd complex is consolidated *through* the intramolecular and intermolecular contacts that are formed between C–H⋯N, C–H⋯O and N–H⋯N. While an intermolecular interaction (C5–H5⋯O1^i, with symmetry code $i = x, y, 1 + z$) contributing to crystal packing was detected in the H$_2$L^4 ligand, three intermolecular connections (C4–H4⋯O2 ^{ii}, C20–H20⋯O2 ^{iii} and C29–H29C⋯O1 ^{iv}, with symmetry codes $ii = x, 2-y, -1/2 + z$; $iii = 1/2-x, 3/2-y, 1-z$; $iv = x, 1-y, 1/2 + z$) were found in the Pd complex. The crystal packing of the pincer ligand H$_2$L^4 and the Pd complex 4 are illustrated in Fig. 2a (H$_2$L^4) and 2b (Complex 4). The intramolecular and intermolecular interactions of the H$_2$L^4 and Pd complex 4 are illustrated in Fig. 3a (H$_2$L^4) and 3b (Complex 4) and Fig. 4 a (H$_2$L^4) and 4b (Complex 4), respectively, and the parameters of the intermolecular and intramolecular H-bonds for the H$_2$L^4 and complex 4 are given in Table 3.

The pincer ligand H$_2$L^4 contains intermolecular ring interactions, which are in the offset *face-to-face* manner. The convenient π⋯π contacts are generally described with interplanar distances between 3.3 and 3.8 Å and the displacement angle up to 20° [50,51]. The acceptable π⋯π interactions in H$_2$L^4 occurred between the Cg(1)⋯Cg(2)^i 3.885(2) Å (Symmetry code: $i = 1-x, 1-y, 1-z$) and Cg(3)⋯Cg (3)^v 3.8087(18) Å (Symmetry code: $v = -x, 1-y, -z$) with displacement angles 22.2 and 24.9°, respectively. Other π⋯π interactions found in H$_2$L^4 are above 3.8 Å and show weaker interactions. The detailed geometrical data of π⋯π interactions of the H$_2$L^4 ligand is listed in

Table 1
Crystal structure refinement parameters of the H$_2$L^4 and complex 4.

Parameters	H$_2$L^4	Complex 4
Empirical formula	C$_{27}$H$_{31}$N$_3$O$_2$	C$_{29}$H$_{32}$N$_4$O$_2$Pd
Formula weight	429.55	574.98
Temperature	273.15 K	298.15 K
Crystal system	Monoclinic	Monoclinic
Space group	$P2_1/c$	$C2/c$
a	12.8772(5) Å	28.276(5) Å
b	14.1350(6) Å	15.649(2) Å
c	13.0122(5) Å	14.735(2) Å
$β$	91.093(2)°	112.481(9)°
Volume	2368.04(16) Å^3	6024.7(16) Å^3
Z	4	8
ρ	1.205 g/cm^3	1.268 g/cm^3
μ	0.604 mm^{-1}	5.196 mm^{-1}
F(000)	920.0	2368.0
Crystal size	0.317 × 0.297 × 0.156 mm^3	0.295 × 0.276 × 0.134 mm^3
Radiation	CuKα (λ = 1.54178 Å)	CuKα (λ = 1.54178 Å)
2Θ range for data collection	6.866°–136.464°	6.584°–136.48°
Index ranges	$-15 ≤ h ≤ 15, -16 ≤ k ≤ 17, -15 ≤ l ≤ 15$	$-34 ≤ h ≤ 34, -18 ≤ k ≤ 17, -17 ≤ l ≤ 17$
Reflections collected	13492	47331
Independent reflections	4292 [R$_{int}$ = 0.1523, R$_{sigma}$ = 0.1227]	5508 [R$_{int}$ = 0.1209, R$_{sigma}$ = 0.0515]
Data/restraints/parameters	4292/0/296	5508/0/333
Goodness-of-fit on F^2	1.029	1.065
Final R indexes [I ≥ 2σ (I)]	R$_1$ = 0.0935, wR$_2$ = 0.2287	R$_1$ = 0.0607, wR$_2$ = 0.1611
Final R indexes [all data]	R$_1$ = 0.1547, wR$_2$ = 0.2685	R$_1$ = 0.0792, wR$_2$ = 0.1749
Largest diff. peak/hole	0.48/-0.43 e.Å^{-3}	0.88/-1.10 e.Å^{-3}
CCDC no*	2259839	2259840

*Supplementary crystallographic data (CCDC 2259839 and 2259840) can be obtained free of charge via https://www.ccdc.cam.ac.uk/structures/.
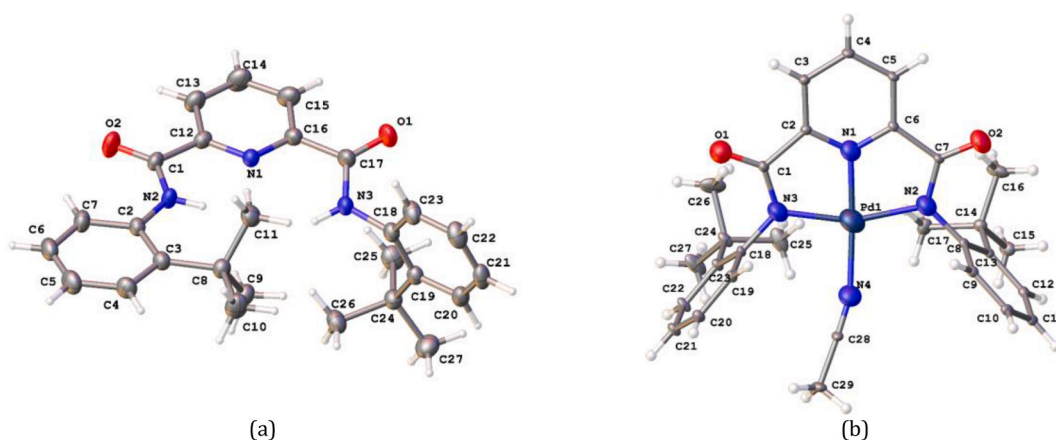
Fig. 1. Crystal structure of (a) H_2L^4 and (b) complex 4.

Table 4 and the Cg···Cg interactions of the H_2L^4 ligand are shown in Fig. 5a.

The C–H ... π interactions comprise the interaction of an aromatic ring's electron-rich π-cloud with a partially positive H atom. According to previous studies, the distance of meaningful C–H···π contact is in the range of 2.8–3.2 Å [52]. Two stacking C–H···π interactions were found in complex 4. These interactions are occurred among the carbon atom of the molecule, which acts a hydrogen bond donor to the centroid of the phenyl ring in the next molecule [53]. The existed C–H···π stacking interactions in complex 4 are C19–H19···Cg(2)[vi] 2.84 Å (Sym: vi = 1/2-x, 3/2-y, 1-z) and C29–H29B···Cg(5)[vii] 2.62 Å (Sym: vii = x, 1-y, 1/2 + z), in addition the C–H···π angles are 147 and 143°, for these interactions, respectively. The C–H···π angles are under the favourable value, which is 180°, and this may be generated from the steric hindrance in the complex [54]. The detailed geometric information of C–H···π stacking contacts of the complex 4 is given in Table 4 and the illustration of the C–H···π stacking contacts of the complex 4 is shown in Fig. 5b.

3.3. UV–Visible study

UV–vis analyses of NNN pincer ligands and their Pd(II) complexes were performed at the 200–800 nm range in acetonitrile at room temperature. An absorption band was determined for the H_2L^2 and H_2L^3 ligands at 278 nm. Although two distinct shoulders were detected in 220 and 280 nm for H_2L^1 and 221 and 268 nm for H_2L^4 spectra, three shoulders were observed at 223, 261, and 309 nm, respectively, for the H_2L^5 ligand. These observed peaks in the ligands are assigned to intraligand n → π* and π → π* transitions in the UV region [27,55]. After complexation, the peaks that were detected in the 220–223 and 261–280 nm range in the ligands were slightly blue-shifted to 218–222 and 260–266 nm in their Pd(II) complex spectra. Furthermore, the new absorption bands that formed between 311 and 321 nm belong to Ligand → Metal charge transfer transitions [56]. The UV absorption spectra of the NNN pincer ligands and their Pd(II) complexes are shown in Fig. 6a and b, respectively.

3.4. Suzuki-Miyaura cross-coupling reaction

To obtain the optimal Suzuki-Miyaura cross-coupling reaction conditions, the effects of solvent, catalyst ratio, base, temperature, and time were examined for the Suzuki-Miyaura cross-coupling reaction in an optimisation study. For this purpose, 4-bromotoluene was used as the substrate and complex 3 as the model catalyst. 0.005 mmol of catalyst **3** was used for preliminary tests. All reactions were performed under aerobic conditions. To find the appropriate base, the reactions were carried out with KOH, K_2CO_3, K_3PO_4, Na_2CO_3, Cs_2CO_3 and Et_3N, as the base and DMF were used as solvent in this stage. At the end of the reaction, K_2CO_3 provided the highest conversion (47.2%, Table 5, entry 2). Among other bases. Although inorganic bases provide varying amounts of conversion, as is known, the least coupling product (2.2% yield, Table 5, entry 6) was obtained when Et_3N, an organic base, was used. As determined in previous studies, potassium-containing bases with a "cation effect" are extremely important for the activation of boronic acid. In addition, being easily accessible and inexpensive has allowed bases such as potassium-containing K_2CO_3 and KOH to be widely used in coupling reactions [57–60]. Optimisation reactions were carried out at 90, 100, 110 and 120 °C, with K_2CO_3 as the base. Since there was no significant difference between 110 and 120 °C (Table 5, entries 9 and 10) according to the conversions and it is also important to perform the reactions under milder conditions, the optimal reaction temperature for the coupling reactions was accepted as 110 °C. DMF, toluene, EtOH, ACN, 1,4-dioxane, H_2O, EtOH–H_2O (v/v: 1:1 mL), 1,4-dioxane-H_2O (v/v = 1:1 mL) were evu, were evulated as solvent, in the presence of K_2CO_3 at 110 °C. EtOH was found to be the best solvent as we obtained a 100% conversion with 98.6% yield (Table 5, Entry 12). In Suzuki C–C coupling reactions, it's crucial to ensure that the catalyst and substrates are as soluble as possible in polar solvents like ethanol [61]. The reactions were then carried out in different time intervals with different mole ratios of the model catalyst under the optimum base, solvent, and temperature determined for the Suzuki-Miyaura cross-coupling reaction. The effect of catalyst amount was investigated, entries 23, 25 and 26 in Table 5, indicate the effect of catalyst loading on the performance of complex 3. When catalyst loading decreased to 0.001 mmol, 86% conversion with 86% yield was obtained in half an hour (Table 5,

Table 2
Selected bond distance (Å) and bond angles, (°) for pincer ligand H_2L^4 and complex 4.

Bond	Distance (Å)	Bond	Angle (°)
N^2,N^6-bis(2-tert-Butylphenyl)pyridine-2,6-dicarboxamide (H_2L^4)			
O1–C17	1.228(4)	C1–N2–C2	130.2(3)
O2–C1	1.213(4)	C12–N1–C16	118.4(2)
N2–C2	1.418(4)	C17–N3–C18	124.0(3)
N2–C1	1.341(4)	C6–C5–C4	120.1(3)
N1–C12	1.330(4)	C5–C6–C7	119.4(4)
N1–C16	1.341(4)	C6–C7–C2	120.9(3)
N3–C17	1.348(4)	C7–C2–N2	119.2(3)
N3–C18	1.427(4)	C7–C2–C3	121.2(3)
C5–C6	1.356(6)	C3–C2–N2	119.6(3)
C5–C4	1.388(5)	O2–C1–N2	126.8(3)
C6–C7	1.382(5)	O2–C1–C12	120.3(3)
C7–C2	1.394(4)	N2–C1–C12	112.8(2)
C2–C3	1.411(4)	N1–C12–C1	117.8(2)
C1–C12	1.512(4)	N1–C12–C13	122.8(3)
C12–C13	1.383(4)	C13–C12–C1	119.4(3)
C16–C17	1.485(4)	N1–C16–C17	117.4(2)
C16–C15	1.393(4)	N1–C16–C15	122.0(3)
C18C19	1.401(4)	C15–C16–C17	120.5(3)
C18–C23	1.382(5)	O1–C17–N3	123.6(3)
C19–C24	1.538(4)	O1–C17–C16	121.6(3)
C19–C20	1.396(4)	N3–C17–C16	114.7(3)
Acetonitrile-N^2,N^6-bis(2-tert-butylphenyl) pyridine-2,6-dicarboxamidopalladium(II) (Complex 4)			
Pd1–N1	1.917(5)	N1–Pd1–N2	80.59(19)
Pd1–N2	2.041(4)	N1–Pd1–N3	81.01(19)
Pd1–N3	2.021(5)	N1–Pd1–N4	174.1(2)
Pd1–N4	2.022(5)	N3–Pd1–N2	161.45(19)
O2–C7	1.220(7)	N3–Pd1–N4	95.8(2)
O1–C1	1.243(7)	N4–Pd1–N2	102.8(2)
N1–C2	1.347(8)	C2–N1–Pd1	117.8(4)
N1–C6	1.334(7)	C6–N1–Pd1	118.3(4)
N2–C7	1.354(7)	C6–N1–C2	123.6(5)
N2–C8	1.444(7)	C7–N2–Pd1	114.6(4)
N3–C18	1.446(7)	C7–N2–C8	120.5(5)
N3–C1	1.336(8)	C8–N2–Pd1	123.8(3)
N4–C28	1.134(8)	C18–N3–Pd1	125.3(4)
C7–C6	1.507(8)	C1–N3–Pd1	114.8(4)
C2–C1	1.513(8)	C1–N3–C18	119.1(5)
C2–C3	1.384(8)	C28–N4–Pd1	162.0(6)
C18–C19	1.373(8)	O2–C7–N2	127.1(6)
C18–C23	1.404(8)	O2–C7–C6	121.0(5)
C6–C5	1.379(8)	N2–C7–C6	111.9(5)
C19–C20	1.383(9)	N1–C2–C1	113.1(5)
C8–C13	1.404(9)	N1–C2–C3	118.9(6)
C4–C3	1.386(9)	N1–C6–C7	114.2(5)
C4–C5	1.385(9)	N1–C6–C5	119.0(6)
C11–C10	1.361(10)	C13–C8–N2	123.8(5)
C23–C22	1.401(9)	C9–C8–N2	114.3(6)

entry 23) and more than 97% conversion with over 97% yield, in 5 h (Table 5, entry 24). When the catalyst loading continued to be reduced, 89% conversion and 89% coupling products were obtained with 0.0002 mmol catalyst in 12 h, while 86% conversion and 86% coupling product were obtained in 12 h when the catalyst ratio was reduced to 0.0001 mmol (Table 5, entries 26 and 25).

Quaternary ammonium salts are known to exert an activating effect on the reaction of arylhalides with phenylboronic acids [62]. Based on this, the effect of tetraethylammonium bromide salt on activity was investigated in this study, but no contribution was observed to increase conversion (Table 5, entry 22).

As a result of the optimisation study with the chosen model catalyst, the optimum base, solvent, time, temperature, and catalyst ratio were investigated for the Suzuki-Miyaura cross-coupling reaction; according to the results the best conditions are identified as follows: K_2CO_3, EtOH, 5 h, 110 °C and 0.001 mmol of catalyst. After the optimum reaction conditions were determined, the activity analyses of the other catalysts were carried out under these determined parameters.

The catalytic activities of the other Pd complexes 1, 2, 4, and 5, which contain different ligand substitutions, were tested under optimised conditions. The results are shown in Table 6. To determine the catalytic activity of Pd complexes, 4-bromotoluene was first used as a substrate in the Suzuki coupling reaction with phenylboronic acid. All palladium complexes were utilized as catalyst in the reaction, conversion rates were determined for each hour, with a maximum of 5 h. All complexes were found to catalyse the coupling of phenylboronic acid with 4-bromotoluene to form the coupling product 4-methylbiphenyl in good yields. In general, the use of
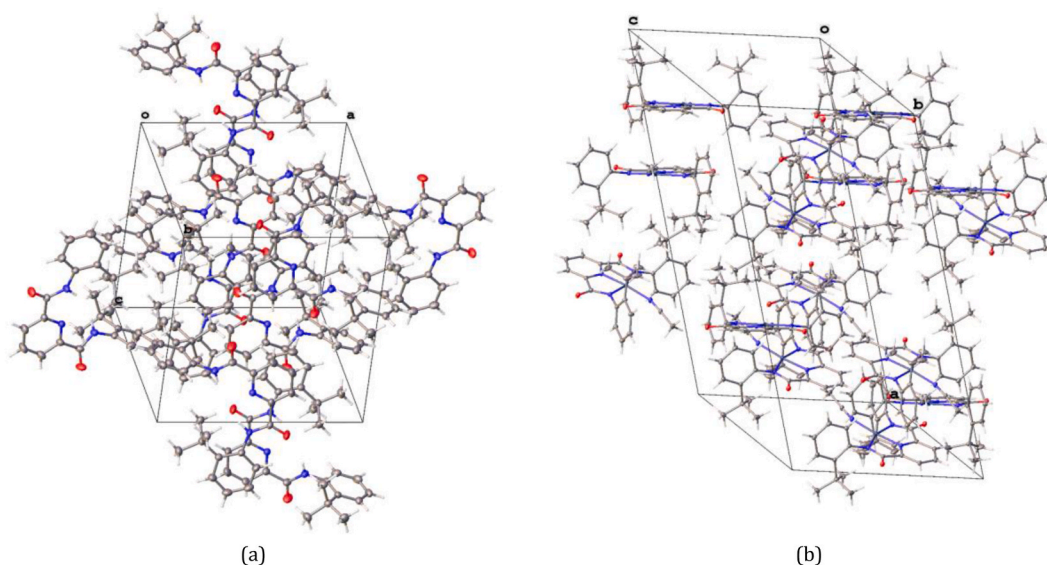
Fig. 2. The crystal packing diagrams of the (a) pincer ligand H$_2$L^4 along the *a*–axis and (b) Pd complex 4 throughout the crystallographic *b*–axis.
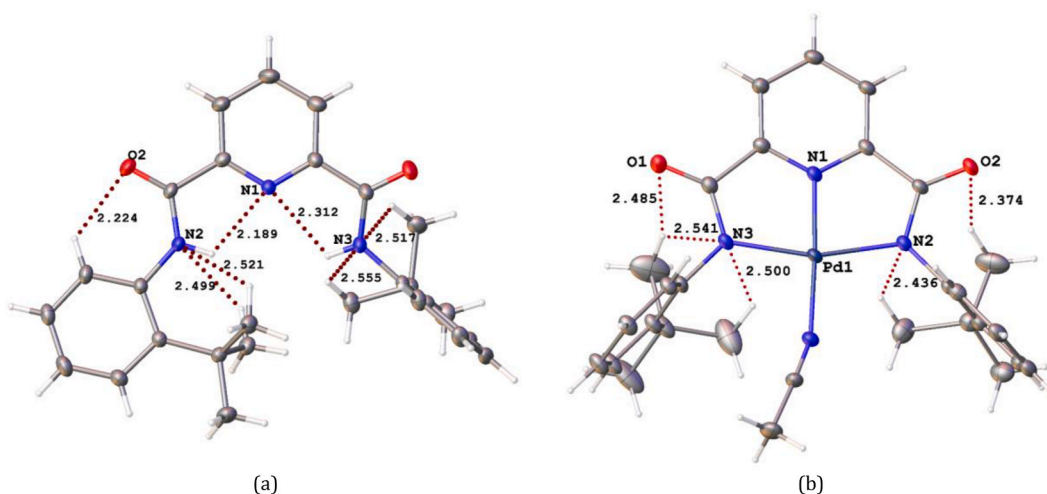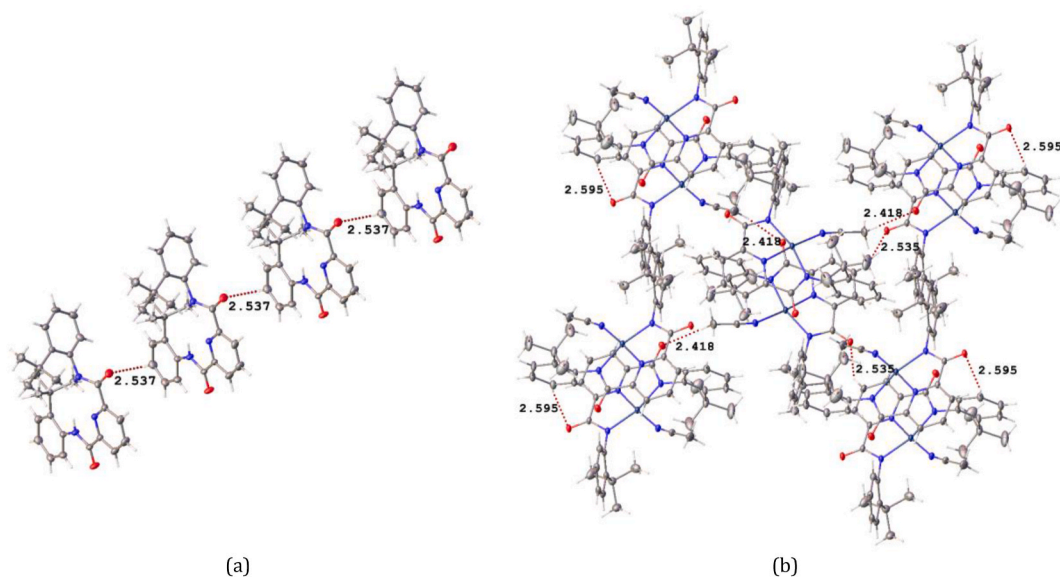

Fig. 3. The intramolecular hydrogen bonds of the (a) H$_2$L^4 and (b) Pd complex 4 generated by the N–H···N, C–H···O, and C–H···N interactions.

deactivated aryl bromides, substituted with electron-donating groups such as -methyl or -methoxy, for the Suzuki C–C coupling reactions decelerates the reaction [63–65]. However, the 1, 2, 4, and 5 Pd complexes which have *ortho*-substituted F, Cl, *tert*-butyl, and NO$_2$ groups, respectively, served as an effective catalyst for the coupling reaction and formed good yields with 4-bromotoluene, which has a donating group at the *para* position on the phenyl ring. In 1 h, 80% conversion with 80% yield and 79% conversion with 79% yield were obtained from 1 to 2 complexes, respectively. The highest conversion and yield of these complexes were obtained at the fourth hour (Table 6, entries 1 and 2). However, there was an increase in the conversion rates provided by these two complexes until the first 4 h, but a slight decrease was observed in the last hour. This is most likely because the catalyst may be saturated after the first 4 h. An excellent yield was achieved from the 4 and 5 complexes, with more than 99% conversion for complex 4 and more than 98% conversion for complex 5 in 1 h (Table 6, entries 3 and 4). Complex 4 contains sterically hindered bulky *tert*-butyl group, which accelerates the oxidative addition of aryl bromides [66]. In the coupling reaction of 4-bromotoluene with phenylboronic acid, the catalytic activity of the 4 and 5 complexes, which provide better conversion than other Pd complexes, was then investigated in coupling reactions using substrates of 1-bromo-4-isobutylbenzene and 2-bromo-6-methoxynaphthalene. The complexes showed good conversion and ensured high yields of coupling products from these bulky deactivated and sterically hindered substrates. In the reaction of 1-bromo-4-isobutyl benzene, complex 4 produced more than 98% conversion and over 98% yield in 1 h (Table 6, entry 5), while complex 5 formed more than 94% conversion and more than 94% coupling product in 1 h (Table 6, entry 6). Furthermore, complex 5 reached more than 96% conversion and generated over 96% yield of the coupling product in 2 h (Table 6, entry 7). In the

Fig. 4. (a) The intermolecular hydrogen bonds via C–H···O interactions led to formation of *zig-zag* motif in H_2L^4 and (b) intermolecular hydrogen bonds generated by the C–H···O contacts in Pd complex 4.

Table 3
Inter molecular and intramolecular hydrogen bonds for H_2L^4 and complex 4 (Å, °) *.

D-H···A	d(D-H)	d(H···A)	d(D···A)	∠ (D-H···A)
H_2L^4				
N2–H2···N1	0.86	2.19	2.654(3)	114
N3–H3···N1	0.86	2.31	2.689 (3)	107
C5–H5···O1^i	0.93	2.54	3.405(5)	155
C7–H7···O2	0.93	2.22	2.871(5)	126
C9–H9C···N2	0.96	2.52	3.162(5)	124
C11–H11A···N2	0.96	2.50	3.109(5)	121
C25–H25B···N3	0.96	2.52	3.131(5)	122
C26–H26B···N3	0.96	2.55	3.163(5)	121
Complex 4				
C4–H4···O2^{ii}	0.93	2.54	3.365(9)	149
C16–H16A···O2	0.96	2.37	3.185(14)	142
C17–H17C···N2	0.96	2.44	3.093(12)	125
C20–H20···O2^{iii}	0.93	2.59	3.363(10)	140
C25–H25A···N3	0.96	2.50	3.165(16)	126
C26–H26C···O1	0.96	2.48	3.392(17)	158
C26–H26C···N3	0.96	2.54	3.218(17)	128
C29–H29C···O1^{iv}	0.96	2.42	3.219(11)	141

*Symmetry code: *i = x, y, 1 + z; ii = x, 2-y, −1/2 + z; iii = 1/2-x, 3/2-y, 1-z; iv = x, 1-y, 1/2 + z.*

Suzuki coupling of 2-bromo-6-methoxynaphthalene, both complexes 4 and 5 gave almost %100 excellent yields in 1 h (Table 6, entries 8 and 9).

As a consequence, the NNN pincer-type-based Pd complexes that we synthesised proved to be very capable in the Suzuki-Miyaura coupling reaction because they exhibited high activity, good selectivity, and excellent yields of the coupling product. When the results obtained in this study are evaluated, it is determined that the catalytic activity of our Pd complexes in the Suzuki-Miyaura coupling reaction was better than the activities of the Pd complexes that have similar NNN ligand structure, which was previously reported by Jerome et al. [44]. Furthermore, the Pd complexes we synthesised as catalysts achieved high conversion in a much shorter time.

3.4.1. Hg poisoning test

The mercury poisoning test is a very significant way to determine whether the reaction is homogeneous or heterogeneous [67]. To understand the nature of the Pd complexes, the Suzuki reaction was performed under optimised conditions. 4-Bromotoluene (1.0 mmol), phenylboronic acid (1.2 mmol), K_2CO_3 (1.2 mmol), EtOH (2 mL), and palladium catalyst (0.001 mmol) and excess Hg (200 molar equivalents of the Pd catalyst) were mixed in a closed reaction tube, and the reaction mixture obtained was stirred for the required time at 110 °C. The procedure for the Suzuki reaction was then repeated, and the isolated yields were analyzed by GC.

Table 4

Geometrical parameters of π···π stacking interactions for H_2L^4 and C–H···π contacts for the complex 4 (Å, °).

H_2L^4

Rings I–J[a,b,l]	Cg(I)···Cg(J)[c]	γ [d]	Cg(I)-perp[e]	Cg(J)-perp[f]	
Cg(1)···Cg(2)[i]	3.885(2)	23.6	3.5599(14)	3.5966(16)	
Cg(1)···Cg(2)[ii]	4.096(2)	30.8	−3.5198(14)	−3.9255(16)	
Cg(2)···Cg(1)[i]	3.885(2)	22.2	3.5966(16)	3.5600(14)	
Cg(2)···Cg(1)[iii]	4.096(2)	16.6	−3.9255(16)	−3.5198(14)	
Cg(3)···Cg(2)[iv]	5.930(2)	72.3	1.8025(16)	3.5276(14)	
Cg(3)···Cg(3)[v]	3.8087(18)	24.9	−3.4559(13)	−3.4558(13)	

Complex 4

C–H···Cg(J)[g]	H···Cg	H-perp[h]	< C–H···Cg[i]	γ [j]	C···Cg[k]
C19 –H19···Cg(2)[vi]	2.84	−2.83	147	5.33	3.649(7)
C29–H29B···Cg(5)[vii]	2.62	−2.58	143	10.64	3.442(10)

[a] H_2L^4: Cg(1), Cg(2) and Cg(3) are the centroid of the rings, (N1–C12–C13–C14–C15–C16), (C2–C7), and (C18–C23), respectively. Complex 4: Cg(2) and Cg(5) are the centroid of the rings, (Pd1–N1–C6–C7–N2) and (C18–C23), respectively.

[b] Ring number I and J (ring number mentioned over).

[c] Centroid margin among ring I and ring J.

[d] Angle among the centroid vector Cg(I)···Cg(J) and the normal to plane J.

[e] Vertical margin of Cg(I) on ring J (Å).

[f] Vertical margin of Cg(J) on ring I (Å).

[g] Center of gravitation of ring J (ring number mentioned over).
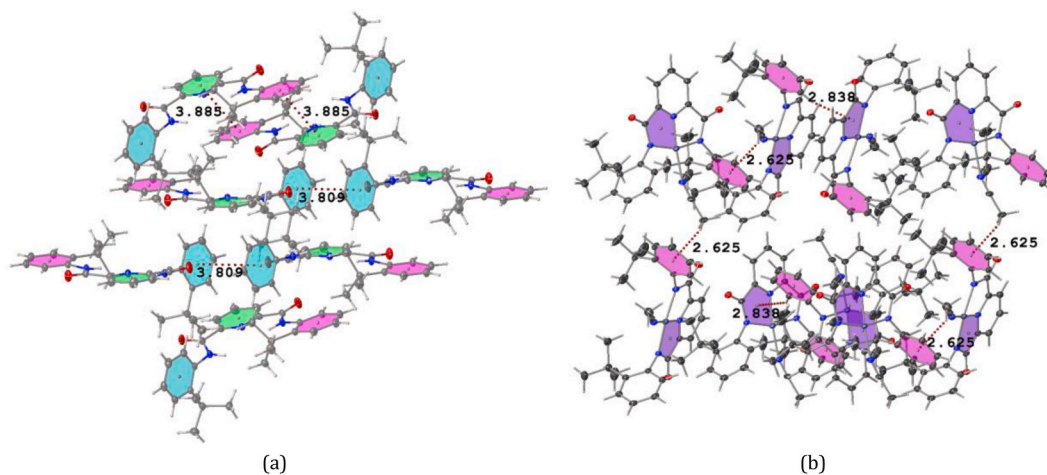
[h] Vertical margin of H to the ring plane J.

[i] Angle among C–H and centroid Cg.

[j] Angle among Cg-H vector and ring J normal.

[k] Margin among C-atom and the proximate carbon atom in the benzene ring.

[l] Symmetry: *i* = 1-*x*, 1-*y*, 1-*z*; *ii* = *x*, 1/2-*y*, −1/2+ *z*; *iii* = *x*, 1/2-*y*, 1/2 + *z*; *iv* = -*x*, 1-*y*, 1-*z*; *v* = -*x*, 1-*y*, -*z*; *vi* = 1/2-*x*, 3/2-*y*, 1-*z*; *vii* = *x*, 1-*y*, 1/2 + *z*.

(a)   (b)

Fig. 5. (a) π···π interactions in H_2L^4 and (b) C–H···π contacts for complex 4.

The Hg (0) poisoning test is the most well-known test to reveal the nature of the complexes and is easy to perform on C–C coupling reactions. Hg(0) amalgamates connect very strongly with Pd(0), Rh(0), and Ni(0) based complexes, thus blocking the access of the active site to the substrate [63,67]. According to the results of the mercury test, when the conversion rates of the complexes are examined, it is seen that there is a serious decrease, although not completely suppressed (Table 7). These findings suggest that catalytic activity is produced by Pd complexes containing the NNN pincer ligand. Because the Pd(0) species are protected by the ligand, the Hg (0) could not fully extinguish the reaction. However, the fact that Hg(0) does not completely stop the reaction and causes extremely low conversions under the same conditions can be explained by ligand dissociation [68]. It is important to point that, studies have reported, not only colloidal Pd(0) but also molecular Pd(0) complexes can be exterminated by elemental mercury [69,70]. Furthermore, Hg(0) poisoning experiments indicate that soluble Pd(0) species are most likely decomposition products of palladacyclines. Therefore, it can be said that catalytic process based on a homogeneous catalytic mechanism including intermediates Pd(0) and Pd(II) [71].

The formed ligand-free molecular paladium species continued to react with Hg until these catalytic species were deactivated [72].
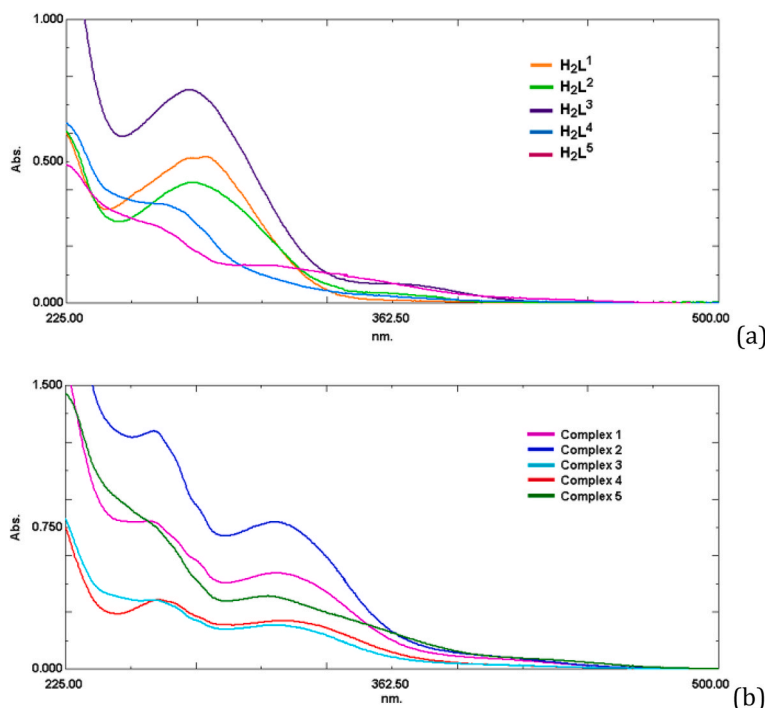
Fig. 6. The superposed UV spectrum of the (a) ligands (H_2L^{1-5}) and (b) Pd(II) complexes in CH_3CN.
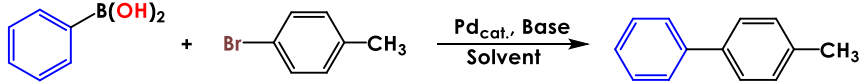
Therefore, ligand-free species or colloids are likely to be active species for the catalytic reaction [73]. These results have shown that NNN ligands in the structures of Pd complexes are extremely important for the stabilization of active catalytic species. At the same time, NNN Pd complexes are intermediate substances required for the generation of effective Pd(0) species in the reaction condition [63,69,74].

3.4.2. Reusability analysis

According to the results of the Hg test, Complex 5 showed a significant decrease in conversion rate. As a result of this, it has been determined that Complex 5, with its more heterogeneous character, is more suitable for the reusability test. For this purpose, the catalytic activity of the black precipitates formed during the reaction of Complex 5 was investigated under optimised conditions for the reusability test. The procedure for the reusability test is as follows; after each cycle was completed, the mixture was diluted with EtOAc (15 mL) and the black precipitates obtained were collected by centrifugation and subsequently rinsed with methanol, water, and diethylether, respectively. Then, dried at 80 °C before using for the next reaction with fresh 4-bromotoluene and phenylboronic acid [41,75,76]. After four cycles, we observed a considerably decrease in the activity of the complex (from %87 conversion for the first run to %34 conversion for the fourth run). In fact, the black residues formed at the end of each reaction could be obtained under very difficult conditions with a significant loss of yield. These results showed how important NNN-pincer ligands are to the catalytic activity of our Pd complexes, considering their role in stabilising the catalytic species formed in the reaction medium. TEM analysis was performed for the morphological characterisation of the resulting black residues. TEM images obtained from the fourth cycle (Fig. 7a and b) indicate that the Pd species are well dispersed. Furthermore, Complex 5 contains nanosized spherical particles.

4. Conclusions

The NNN pincer-type novel five-ligand and their Pd(II) complexes were synthesised and characterised with several methods. The crystal structure of one ligand and its Pd(II) complex (H_2L^4 and complex 4) was also able to be elucidated with a single-crystal XRD analysis. The single-crystal XRD data provided us to better understand the molecular structures of the NNN pincer ligand and its Pd complex. Single crystal XRD results revealed that both the ligand and its Pd complex contain supramolecular interactions. These intramolecular and intermolecular contacts that are formed between C–H···N, C–H···O, N–H···N, π···π and C–H … π are contributing to stabilization of the crystal system. In line with previous studies in the literature, pincer complexes are known to be effective in C–C cross-coupling reactions. On the basis of all of these studies, the catalytic activities of the synthesised Pd(II) complexes were tested in the Suzuki-Miyaura cross-coupling reaction. According to the results of the catalytic study, it was determined that our pincer-structured Pd(II) complexes were highly capable of the Suzuki C–C cross-coupling reaction between the sterically hindered and deactivated aryl bromides and phenylbronic acid at the required reaction times. Furthermore, these Pd(II) complexes demonstrated good conversion and selectivity at short times with even low catalyst loadings. Among the synthesised complexes, when evaluated on

Table 5
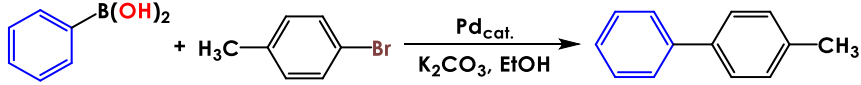The obtained optimisation parameters for the Suzuki C–C coupling reaction[a].

Entry	Catalyst (mmol)	Base	Solvent	Temperature (°C)	Time (h)	Conversion (%)[b]	Yield (%)[b]	Selectivity (%)	TON[c]
1	0.005	KOH	DMF	80	12	>13	>1	>11	>27
2	0.005	K_2CO_3	DMF	80	12	>47	>28	>60	>94
3	0.005	K_3PO_4	DMF	80	12	>14	>1	>11	>28
4	0.005	Na_2CO_3	DMF	80	12	>41	>20	>48	>83
5	0.005	Cs_2CO_3	DMF	80	12	>13	>0	>3	>27
6	0.005	Et_3N	DMF	80	12	>43	>2	>5	>87
7	0.005	K_2CO_3	DMF	90	12	>46	28	>60	>92
8	0.005	K_2CO_3	DMF	100	12	>50	>35	>65	>100
9	0.005	K_2CO_3	DMF	110	12	51	36	70	102
10	0.005	K_2CO_3	DMF	120	12	52	36	69	104
11	0.005	K_2CO_3	H_2O	110	12	82	>76	>93	164
12	0.005	K_2CO_3	EtOH	110	12	100	>98	>98	200
13	0.005	K_2CO_3	1,4-Dioxane	110	12	91	>85	94	182
14	0.005	K_2CO_3	Toluene	110	12	>98	>92	>93	>197
15	0.005	K_2CO_3	CH_3CN	110	12	100	94	94	200
16	0.005	K_2CO_3	Et_4NBr-DMF	110	12	>58	>49	84	>197
17	0.005	K_2CO_3	EtOH– H_2O	110	12	100	>94	>94	200
18	0.005	K_2CO_3	1,4-Dioxane-H_2O	110	12	>97	>94	>97	>194
19	0.005	K_2CO_3	EtOH	110	2	96	95	>98	192
20	0.005	K_2CO_3	EtOH–Et_4NBr	110	2	98	97[d]	>98	196
21	0.005	K_2CO_3	EtOH	110	4	98	97	>98	196
22	0.005	K_2CO_3	EtOH–Et_4NBr	110	4	98	97[d]	>98	196
23	0.001	K_2CO_3	EtOH	110	0.5	86	86	100	860
24	0.001	K_2CO_3	EtOH	110	5	>97	>97	100	>970
25	0.0001	K_2CO_3	EtOH	110	12	86	86	100	8600
26	0.0002	K_2CO_3	EtOH	110	12	89	89	100	4450

[a] Reaction circumstances: 4-Bromotoluene (1.0 mmol), phenylboronic acid (1.2 mmol), base (1.2 mmol), solvent (2 mL).
[b] Yield and conversion rates were determined by GC analysis based on aryl halides in the presence of dodecane used as internal standard.
[c] Mole product/mole catalyst.
[d] Et_4NBr (0.02 mmol).

Table 6
The catalytic activities of NNN Pd pincer complexes in Suzuki-Miyaura C–C coupling reaction[a].

$$Ar\text{-}Br + Ph\text{-}B(OH)_2 \longrightarrow Ar\text{-}Ph$$

Entry	Catalyst	Substrate	Time (h)	Conversion (%)[b]	Yield (%)[b]	TON[c]
1	Complex 1	4-Bromotoluene	4	>91	>91	>910
2	Complex 2	4-Bromotoluene	4	>93	>93	>930
3	Complex 4	4-Bromotoluene	1	>99	>99	>990
4	Complex 5	4-Bromotoluene	1	>98	>98	>980
5	Complex 4	1-Bromo-4-izobutylbenzene	1	>98	>98	>980
6	Complex 5	1-Bromo-4-izobutylbenzene	1	>94	>94	>940
7	Complex 5	1-Bromo-4-izobutylbenzene	2	>96	>96	>960
8	Complex 4	2-Bromo-6-methoxynaphthalene	1	100	>99	1000
9	Complex 5	2-Bromo-6-methoxynaphthalene	1	100	>99	1000

[a] Reaction circumstances: Ar–Br (1.0 mmol), phenylboronic acid (1.2 mmol), K_2CO_3 (1.2 mmol), catalysis (0.001 mmol), EtOH (2 mL) at 110 °C.
[b] Yield and conversion rates were determined by GC analysis based on aryl halides in the presence of dodecane used as internal standard.
[c] Mole product/mole catalyst.

the basis of their high conversion and selectivity that they showed in short time periods, it was determined that complexes 4 and 5 performed higher activity. For example, complete conversion and nearly 100% yield were achieved from the reaction of the 2-bromo-6-methoxynaphthalene substrate with phenylboronic acid, which Complex 4 and 5 used as catalyst. Reusability analysis was performed with the black residues of complex 5. Unfortunately, progressively lower conversion rates were obtained as a result of each cycle (from %87 conversion for the first run to %34 conversion for the fourth run). On the basis of the results of the Hg(0) poisoning test, although a serious decrease in the activity of all Pd(II) complexes was observed, it was not completely suppressed, and the reaction continued at a certain conversion rate. This showed us that our NNN pincer-type ligands are extremely important in terms of stabilising the active catalytic species formed during the reaction in the medium and are also the distributors of the generated active particles. To

Table 7

Activation of catalysts in Suzuki-Miyaura coupling reaction between 4-bromotoluene and phenylboronic acid under Hg(0) poisoning effect[a].

Entry	Catalyst	Time (h)	Conversion (%)[b]	Yield (%)[b]	TON[c]
1	Complex 1	4	>18	>16	>180
2	Complex 2	4	>38	>36	>380
3	Complex 3	5	>37	>34	>370
4	Complex 4	1	>39	>39	>390
5	Complex 5	1	>16	>16	>160

[a] Reaction circumstances: Ar–Br (1.0 mmol), phenylboronic acid (1.2 mmol), K_2CO_3 (1.2 mmol), catalysis (0.001 mmol), EtOH (2 mL) and Hg (200 molar equivalents of the Pd catalyst) at 110 °C.

[b] Yield and conversion rates were determined by GC analysis based on aryl halides in the presence of dodecane used as internal standard.

[c] Mole product/mole catalyst.
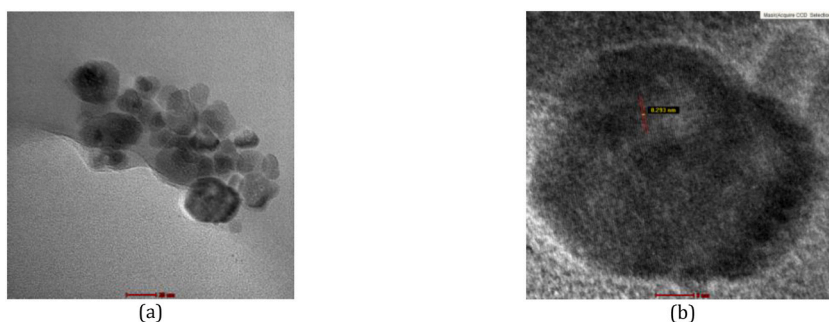
Fig. 7. TEM images for complex 5 at (a) 20 nm and (b) 5 nm scales.

contribute to the number of catalytic studies in the scope of cross-coupling reactions, in our current studies, the synthesis of these and similar pincer complexes and their catalytic applicability in various catalytic reactions continues to be investigated.

Authorship contribution statement

Hakan Arslan: Conceived and designed the experiments; Performed the experiments; Analyzed and interpreted the data; Contributed reagents, materials, analysis tools or data; Wrote the paper.

Ebru Keskin: Performed the experiments; Analyzed and interpreted the data; Contributed reagents, materials, analysis tools or data; Wrote the paper.

Data availability statement

Data will be made available on request.

Declaration of competing interest

The authors declare that they have no known competing financial interests or personal relationships that could have appeared to influence the work reported in this paper.

Appendix A. Supplementary data

Supplementary data to this article can be found online at https://doi.org/10.1016/j.heliyon.2023.e17608.

References

[1] V.N. Shinde, N. Bhuvanesh, A. Kumar, H. Joshi, Design and syntheses of palladium complexes of NNN/CNN pincer ligands: catalyst for cross dehydrogenative coupling reaction of heteroarenes, Organometallics 39 (2020) 324–333, https://doi.org/10.1021/acs.organomet.9b00695.

[2] A. Suzuki, Cross-coupling reactions of organoboranes: an easy way to construct C-C bonds (Nobel Lecture), Angew Chem. Int. Ed. Engl. 50 (2011) 6722–6737, https://doi.org/10.1002/anie.201101379.

[3] M.C. D'Alterio, È. Casals-Cruañas, N.V. Tzouras, G. Talarico, S.P. Nolan, A. Poater, Mechanistic aspects of the palladium-catalyzed Suzuki-Miyaura cross-coupling reaction, Chemistry 27 (2021) 13481–13493, https://doi.org/10.1002/chem.202101880.

[4] C.M. Frech, L.J.W. Shimon, D. Milstein, Redox-induced collapse and regeneration of a pincer-type complex framework: a nonplanar coordination mode of palladium(II), Angew. Chem. Int. Ed. 44 (2005) 1709–1711, https://doi.org/10.1002/anie.200462386.

[5] L.T. Pilarski, N. Selander, D. Böse, K.J. Szabó, Catalytic allylic C-H acetoxylation and benzoyloxylation via suggested (η3-Allyl)palladium(IV) intermediates, Org. Lett. 11 (23) (2009) 5518–5521, https://doi.org/10.1021/ol9023369.

[6] M. Ohff, A. Ohff, M.E. van der Boom, D. Milstein, Highly active Pd(II) PCP-type catalysts for the heck reaction, J. Am. Chem. Soc. 119 (1997) 11687–11688, https://doi.org/10.1021/ja972969z.

[7] M. Asay, D. Morales-Morales, Recent advances on the chemistry of POCOP–nickel pincer compounds, in: Topics in Organometallic Chemistry, vol. 54, Springer, Cham, 2015, https://doi.org/10.1007/3418_2015_135.

[8] J. Aydin, J.M. Larsson, N. Selander, K.J. Szabó, Pincer complex-catalyzed redox coupling of alkenes with iodonium salts via presumed palladium(IV) intermediates, Org. Lett. 11 (13) (2009) 2852–2854, https://doi.org/10.1021/ol9010739.

[9] N. Selander, K. J Szabó, Catalysis by palladium pincer complexes, Chem. Rev. 111 (2011) 2048–2076, https://doi.org/10.1021/cr1002112.

[10] E. Balaraman, B. Gnanaprakasam, L.J.W. Shimon, D. Milstein, Direct hydrogenation of amides to alcohols and amines under mild conditions, J. Am. Chem. Soc. 132 (2010) 16756–16758, https://doi.org/10.1021/ja1080019.

[11] R. Barrios-Francisco, E. Balaraman, Y. Diskin-Posner, G. Leitus, L.J.W. Shimon, D. Milstein, PNN ruthenium pincer complexes based on phosphinated 2,2'-dipyridinemethane and 2,2'-oxobispyridine. Metal–ligand cooperation in cyclometalation and catalysis, Organometallics 32 (2013) 2973–2982, https://doi.org/10.1021/om400194w.

[12] D. Spasyuk, S. Smith, D.G. Gusev, From esters to alcohols and back with ruthenium and osmium catalysts, Angew Chem. Int. Ed. Engl. 51 (2012) 2772–2775, https://doi.org/10.1002/anie.201108956.

[13] E. Peris, R.H. Crabtree, Key factors in pincer ligand design, Chem. Soc. Rev. 47 (2018) 1959–1968, https://doi.org/10.1039/c7cs00693d.

[14] L. Gonzalez-Sebastian, D. Morales-Morales, Cross-coupling reactions catalysed by palladium pincer complexes. A review of recent advances, J. Organomet. Chem. 893 (2019) 39–51, https://doi.org/10.1016/j.jorganchem.2019.04.021.

[15] B.M. Ramalingam, I. Ramakrishna, M. Baidya, Nickel-catalyzed direct alkenylation of methyl heteroarenes with primary alcohols, J. Org. Chem. 84 (2019) 9819–9825, https://doi.org/10.1021/acs.joc.9b01517.

[16] S. Meghdadi, M. Amirnasr, A. Amiri, Z. Musavizadeh Mobarakeh, Z. Azarkamanzad, Benign synthesis of N-(8-quinolyl)pyridine-2-carboxamide) ligand (Hbpq), and its Ni(II) and Cu(II) complexes. A fluorescent probe for direct detection of nitric oxide in acetonitrile solution based on Hbpq copper(II) acetate interaction, C. R. Chim. 17 (2014) 477–483, https://doi.org/10.1016/j.crci.2013.10.003.

[17] Z.-H. Ni, H.-Z. Kou, L.-F. Zhang, W.-W. Ni, Y.-B. Jiang, A.-L. Cui, J. Ribas, O. Sato, mer-[Fe(pcq)(CN)$_3$]⁻: a novel cyanide-containing building block and its application to assembling cyanide-bridged trinuclear Fe$_2^{III}$Mn^{II} complexes [pcq⁻ = 8-(pyridine-2-carboxamido)quinoline anion], Inorg. Chem. 44 (2005) 9631–9633, https://doi.org/10.1021/ic051385v.

[18] W. Zhang, Y. Wang, J. Cao, L. Wang, Y. Pan, C. Redshaw, W.-H. Sun, Synthesis and characterization of dialkylaluminum amidates and their ring-opening polymerization of ε-caprolactone, Organometallics 30 (2011) 6253–6261, https://doi.org/10.1021/om2008343.

[19] O.V. Dolomanov, L.J. Bourhis, R.J. Gildea, J.A.K. Howard, H. Puschmann, OLEX2: a complete structure solution, refinement and analysis program, J. Appl. Crystallogr. 42 (2009) 339–341, https://doi.org/10.1107/s0021889808042726.

[20] L. Palatinus, G. Chapuis, SUPERFLIP– a computer program for the solution of crystal structures by charge flipping in arbitrary dimensions, J. Appl. Crystallogr. 40 (2007) 786–790, https://doi.org/10.1107/s0021889807029238.

[21] L. Palatinus, A. van der Lee, Symmetry determination following structure solution inP1, J. Appl. Crystallogr. 41 (2008) 975–984, https://doi.org/10.1107/s0021889808028185.

[22] L. Palatinus, S.J. Prathapa, S. van Smaalen, EDMA: a computer program for topological analysis of discrete electron densities, J. Appl. Crystallogr. 45 (2012) 575–580, https://doi.org/10.1107/s0021889812016068.

[23] G.M. Sheldrick, Crystal structure refinement with SHELXL, Acta Crystallogr. C Struct. Chem. 71 (2015) 3–8, https://doi.org/10.1107/S2053229614024218.

[24] A. Arrieta, J.M. Aizpurua, C. Palomo, N,N-Dimethylchlorosulfitemethaniminium chloride (SOCl2-DMF) a versatile dehydrating reagent, Tetrahedron Lett. 25 (31) (1984) 3365–3368, https://doi.org/10.1016/s0040-4039(01)81386-1.

[25] S. Gu, H. Xu, N. Zhang, W. Chen, Triazole-functionalized N-heterocyclic carbene complexes of palladium and platinum and efficient aqueous Suzuki-Miyaura coupling reaction, Chem. Asian J. 5 (2010) 1677–1686, https://doi.org/10.1002/asia.201000071.

[26] M. Camacho-Espinoza, J.G. Penieres-Carrillo, H. Rios-Guerra, S. Lagunas-Rivera, F. Ortega-Jiménez, An efficient and simple imidazole-hydrazone ligand for palladium-catalyzed Suzuki-Miyaura cross-coupling reactions in water under infrared irradiation, J. Organomet. Chem. 880 (2019) 386–391, https://doi.org/10.1016/j.jorganchem.2018.11.016.

[27] U. Solmaz, S. Ince, M.K. Yilmaz, H. Arslan, Conversion of monodentate benzoylthiourea palladium(II) complex to bidentate coordination mode: synthesis, crystal structure and catalytic activity in the Suzuki-Miyaura cross-coupling reaction, J. Organomet. Chem. 973–974 (2022), 122374, https://doi.org/10.1016/j.jorganchem.2022.122374.

[28] U. Solmaz, H. Arslan, Spectral, crystallographic, theoretical, and catalytic activity studies of the PdII complexes in different coordination modes of benzoylthiourea ligand, J. Mol. Struct. 1269 (2022), 133839, https://doi.org/10.1016/j.molstruc.2022.133839.

[29] E. Keskin, U. Solmaz, I. Gumus, H. Arslan, Di- and tetra-nuclear oxorhenium(V) complexes of benzoylthiourea derivative ligands: synthesis, structural characterization, and catalytic applications, Polyhedron 219 (2022), 115786, https://doi.org/10.1016/j.poly.2022.115786.

[30] U. Solmaz, I. Gumus, G. Binzet, O. Celik, G.K. Balci, A. Dogen, H. Arslan, Synthesis, characterization, crystal structure, and antimicrobial studies of novel thiourea derivative ligands and their platinum complexes, J. Coord. Chem. 71 (2018) 200–218, https://doi.org/10.1080/00958972.2018.1427233.

[31] I. Gumus, U. Solmaz, G. Binzet, E. Keskin, B. Arslan, H. Arslan, Hirshfeld surface analyses and crystal structures of supramolecular self-assembly thiourea derivatives directed by non-covalent interactions, J. Mol. Struct. 1157 (2018) 78–88, https://doi.org/10.1016/j.molstruc.2017.12.017.

[32] I. Gumus, U. Solmaz, O. Celik, G. Binzet, G.K. Balcı, H. Arslan, Synthesis, characterization and crystal structure of cis-bis[4-fluoro-N-(diethylcarbamothioyl) benzamido-κ2O,S]platinum(II), Eur. J. Chem. 6 (2015) 237–241, https://doi.org/10.5155/eurjchem.6.3.237-241.1265.

[33] E. Keskin, U. Solmaz, G. Binzet, I. Gumus, H. Arslan, Synthesis, characterization and crystal structure of platinum(II) complexes with thiourea derivative ligands, Eur. J. Chem. 9 (2018) 360–368, https://doi.org/10.5155/eurjchem.9.4.360-368.1774.

[34] I. Gumus, S. Gonca, B. Arslan, E. Keskin, U. Solmaz, H. Arslan, N-(Dibenzylcarbamothioyl)-3-methylbutanamide: crystal structure, Hirshfeld surfaces and antimicrobial activity, Eur. J. Chem. 8 (2017) 410–416, https://doi.org/10.5155/eurjchem.8.4.410-416.1650.

[35] U. Solmaz, E. Keskin, I. Gumus, P.K. Cevik, G. Binzet, H. Arslan, Platinum(ii) complex containing n-(*bis*(-2,4-dimethoxy-benzyl)carbamothioyl)- 4-methyl-benzamide ligand: synthesis, crystal structure, Hirshfeld surface analysis, and antimicrobial activity, J. Struct. Chem. 63 (2022) 62–74, https://doi.org/10.1134/s0022476622010073.

[36] I. Gumus, U. Solmaz, S. Gonca, H. Arslan, Molecular self-assembly in indole-based benzamide derivative: crystal structure, Hirshfeld surfaces and antimicrobial activity, Eur. J. Chem. 8 (2017) 349–357, https://doi.org/10.5155/eurjchem.8.4.349-357.1637.

[37] C.K. Ozer, U. Solmaz, H. Arslan, Crystal structure, Hirshfeld surface analysis, and DFT studies of N-(2-chlorophenylcarbamothioyl)cyclohexanecarboxamide, Eur. J. Chem. 12 (2021) 439–449, https://doi.org/10.5155/eurjchem.12.4.439-449.2196.

[38] E. Keskin, E. Turunc, H. Arslan, Synthesis, characterization, electrochemical behavior, and catalytic activity of cobalt(II) metal complexes with pincer-type methylbenzamide derivative ligands, Polyhedron 221 (2022), 115846, https://doi.org/10.1016/j.poly.2022.115846.

[39] B. Arslan, G. Binzet, Synthesis, crystal structure analysis, DFT calculations, antioxidant and antimicrobial activity of *N,N*-di-2,4-dimethoxybenzyl-*N'*-2-nitrobenzoylthiourea, J. Mol. Struct. 1267 (2022), 133579, https://doi.org/10.1016/j.molstruc.2022.133579.

[40] M. Ilis, D. Batalu, I. Pasuk, V. Cîrcu, Cyclometalated palladium(II) metallomesogens with Schiff bases and *N*-benzoyl thiourea derivatives as co-ligands, J. Mol. Liq. 233 (2017) 45–51, https://doi.org/10.1016/j.molliq.2017.02.114.

[41] U. Solmaz, I. Gumus, M. Yilmaz, S. Ince, H. Arslan, Palladium complexes derived from benzoylthiourea ligands: synthesis, crystal structure, and catalytic application in Suzuki C–C coupling reactions, Appl. Organomet. Chem. 35 (2021), https://doi.org/10.1002/aoc.6348.

[42] R.A. Lal, S. Choudhury, A. Ahmed, R. Borthakur, M. Asthana, A. Kumar, Synthesis of homobimetallic molybdenum(VI) complex of *bis*(2-hydroxy-1-naphthaldehyde)malonoyldihydrazone and its reaction with electron and proton bases, Spectrochim. Acta Mol. Biomol. Spectrosc. 75 (2010) 212–224, https://doi.org/10.1016/j.saa.2009.10.014.

[43] Q.-Q. Wang, R.A. Begum, V.W. Day, K. Bowman-James, Chemical mustard containment using simple palladium pincer complexes: the influence of molecular walls, J. Am. Chem. Soc. 135 (2013) 17193–17199, https://doi.org/10.1021/ja408770u.

[44] P. Jerome, P.N. Sathishkumar, N.S.P. Bhuvanesh, R. Karvembu, Towards phosphine-free Pd(II) pincer complexes for catalyzing Suzuki-Miyaura cross-coupling reaction in aqueous medium, J. Organomet. Chem. 845 (2017) 115–124, https://doi.org/10.1016/j.jorganchem.2017.03.045.

[45] F.H. Allen, O. Kennard, D.G. Watson, L. Brammer, A.G. Orpen, R. Taylor, Tables of bond lengths determined by *X*-ray and neutron diffraction. Part 1. Bond lengths in organic compounds, J. Chem. Soc., Perkin Trans. 2 (1987) S1–S19, https://doi.org/10.1039/P298700000S1.

[46] H. Arslan, N. Külcü, U. Flörke, Synthesis and characterization of copper(II), nickel(II) and cobalt(II) complexes with novel thiourea derivatives, Transit. Met. Chem. 28 (2003) 816–819, https://doi.org/10.1023/a:1026064232260.

[47] J. Cirera, P. Alemany, S. Alvarez, Mapping the stereochemistry and symmetry of tetracoordinate transition-metal complexes, Chemistry 10 (2004) 190–207, https://doi.org/10.1002/chem.200305074.

[48] L. Latheef, M.R. Prathapachandra Kurup, Spectral and structural studies of nickel(II) complexes of salicylaldehyde 3-azacyclothiosemicarbazones, Polyhedron 27 (2008) 35–43, https://doi.org/10.1016/j.poly.2007.08.048.

[49] S. Yadav, A. Singh, N. Rashid, M. Ghotia, T.K. Roy, P.P. Ingole, S. Ray, S.M. Mobin, C. Dash, Phosphine-free bis(pyrrolyl)pyridine based NNN-pincer palladium (II) complexes as efficient catalysts for Suzuki-miyaura cross-coupling reactions of aryl bromides in aqueous medium, ChemistrySelect 3 (2018) 9469–9475, https://doi.org/10.1002/slct.201801647.

[50] L. Yang, D.R. Powell, R.P. Houser, Structural variation in copper(I) complexes with pyridylmethylamide ligands: structural analysis with a new four-coordinate geometry index, τ₄, Dalton Trans. (2007) 955–964, https://doi.org/10.1039/b617136b.

[51] C. Janiak, A critical account on π–π stacking in metal complexes with aromatic nitrogen-containing ligands, J. Chem. Soc. Dalton Trans. (2000) 3885–3896, https://doi.org/10.1039/B003010O.

[52] S. Roy, M.G.B. Drew, A. Bauzá, A. Frontera, S. Chattopadhyay, Estimation of conventional C–H···π (arene), unconventional C–H···π (chelate) and C–H···π (thiocyanate) interactions in hetero-nuclear nickel(ii)–cadmium(ii) complexes with a compartmental Schiff base, Dalton Trans. 46 (2017) 5384–5397, https://doi.org/10.1039/c6dt04906k.

[53] I. Gumus, U. Solmaz, G. Binzet, E. Keskin, B. Arslan, H. Arslan, Supramolecular self-assembly of new thiourea derivatives directed by intermolecular hydrogen bonds and weak interactions: crystal structures and Hirshfeld surface analysis, Res. Chem. Intermed. 45 (2019) 169–198, https://doi.org/10.1007/s11164-018-3596-5.

[54] Y.-F. Jiang, C.-J. Xi, Y.-Z. Liu, J. Niclós-Gutiérrez, D. Choquesillo-Lazarte, Intramolecular "CH···π(metal chelate ring) interactions" as structural evidence for metalloaromaticity in bis(pyridine-2,6-diimine)Ru II complexes: intramolecular interactions as evidence for metalloaromaticity, 2005, Eur. J. Inorg. Chem. (2005) 1585–1588, https://doi.org/10.1002/ejic.200400864.

[55] R.A. Pratiwi, A.B.D. Nandiyanto, How to read and interpret UV-VIS spectrophotometric results in determining the structure of chemical compounds, Indonesian J. Edu. Res. Technol. 2 (1) (2022), https://doi.org/10.17509/ijert.v2i1.35171, 1–20.

[56] A. Akbari, Z. Alinia, Synthesis, characterization, and DFT calculation of a Pd(II) Schiff base complex, Turk. J. Chem. 37 (2013) 867–878, https://doi.org/10.3906/kim-1207-74.

[57] A. Scrivanti, M. Bertoldini, U. Matteoli, S. Antonaroli, B. Crociani, [PdCl₂{8-(di-*tert*-butylphosphinooxy)quinoline)}]: a highly efficient catalyst for Suzuki–Miyaura reaction, Tetrahedron 65 (2009) 7611–7615, https://doi.org/10.1016/j.tet.2009.06.099.

[58] R.B. Bedford, S.L. Hazelwood, neé Welch), P.N. Horton, M.B. Hursthouse, Orthopalladated phosphinite complexes as high-activity catalysts for the Suzuki reaction, Dalton Trans. 21 (2003) 4164–4174, https://doi.org/10.1039/B303657J.

[59] R.B. Bedford, S.L. Hazelwood, M.E. Limmert, D.A. Albisson, S.M. Draper, P.N. Scully, S.J. Coles, M.B. Hursthouse, Orthopalladated and -platinated bulky triarylphosphite complexes: synthesis, reactivity and application as high-activity catalysts for Suzuki and Stille coupling reactions, Chemistry 9 (2003) 3216–3227, https://doi.org/10.1002/chem.200304997.

[60] C.M. So, C.C. Yeung, C.P. Lau, F.Y. Kwong, A new family of tunable indolylphosphine ligands by one-pot assembly and their applications in Suzuki-Miyaura coupling of aryl chlorides, J. Org. Chem. 73 (2008) 7803–7806, https://doi.org/10.1021/jo801544w.

[61] A. Wolfson, S. Biton, O. Levy-Ontman, Study of Pd-based catalysts within red algae-derived polysaccharide supports in a Suzuki cross-coupling reaction, RSC Adv. 8 (2018) 37939–37948, https://doi.org/10.1039/c8ra08408d.

[62] K. Selvakumar, A. Zapf, M. Beller, New palladium carbene catalysts for the Heck reaction of aryl chlorides in ionic liquids, Org. Lett. 4 (2002) 3031–3033, https://doi.org/10.1021/ol020103h.

[63] T. Mahamo, M.M. Mogorosi, J.R. Moss, S.F. Mapolie, K. Lammertsma, G.S. Smith, Neutral palladium(II) complexes with P,N Schiff-base ligands: synthesis, characterization and application as Suzuki–Miyaura coupling catalysts, J. Organomet. Chem. 703 (2012) 34–42, https://doi.org/10.1016/j.jorganchem.2011.12.021.

[64] M.K. Yilmaz, Palladium(II) complexes with new bidentate phosphine-imine ligands for the Suzuki C C coupling reactions in supercritical carbon dioxide, J. Supercrit. Fluids 138 (2018) 221–227, https://doi.org/10.1016/j.supflu.2018.04.022.

[65] M.K. Yılmaz, B. Güzel, Iminophosphine palladium(II) complexes: synthesis, characterization, and application in Heck cross-coupling reaction of aryl bromides: heck cross-coupling reactions with iminophosphine Pd(II) complexes, Appl. Organomet. Chem. 28 (2014) 529–536, https://doi.org/10.1002/aoc.3158.

[66] M. Ulusoy, Ö. Birel, O. Şahin, O. Büyükgüngör, B. Cetinkaya, Structural, spectral, electrochemical and catalytic reactivity studies of a series of N₂O₂ chelated palladium(II) complexes, Polyhedron 38 (2012) 141–148, https://doi.org/10.1016/j.poly.2012.02.035.

[67] A. Şengül, M.E. Hanhan, Water soluble benzimidazole containing ionic palladium(II) complex for rapid microwave-assisted Suzuki reaction of aryl chlorides: water soluble benzimidazole - Pd(II) complexes for Suzuki reaction, Appl. Organomet. Chem. 32 (2018) e4288, https://doi.org/10.1002/aoc.4288.

[68] S.M. Nobre, A.L. Monteiro, Pd complexes of iminophosphine ligands: a homogeneous molecular catalyst for Suzuki–Miyaura cross-coupling reactions under mild conditions, J. Mol. Catal. Chem. 313 (2009) 65–73, https://doi.org/10.1016/j.molcata.2009.08.003.

[69] D. Olsson, O.F. Wendt, Suzuki reaction catalysed by a PCsp3P pincer Pd(II) complex: evidence for a mechanism involving molecular species, J. Organomet. Chem. 694 (2009) 3112–3115, https://doi.org/10.1016/j.jorganchem.2009.05.025.

[70] R. van Asselt, C.J. Elsevier, Homogeneous catalytic hydrogenation of alkenes by zero-valent palladium complexes of *cis*-fixed dinitrogen ligands, J. Mol. Catal. 65 (1991), https://doi.org/10.1016/0304-5102(91)85057-9. L13–L19.

[71] S.J. Sabounchei, M. Ahmadi, M. Panahimehr, F.A. Bagherjeri, Z. Nasri, Phosphine mono- and bis-ylide palladacycles as homogeneous molecular precatalysts: simple and efficient protocol greatly facilitate Suzuki and Heck coupling reactions, J. Mol. Catal. Chem. (2014) 383–384, https://doi.org/10.1016/j.molcata.2014.01.002, 249–259.

[72] N.T.S. Phan, M. Van Der Sluys, C.W. Jones, On the nature of the active species in palladium catalyzed mizoroki–heck and Suzuki–miyaura couplings – homogeneous or heterogeneous catalysis, A critical review, Adv. Synth. Catal. 348 (2006) 609–679, https://doi.org/10.1002/adsc.200505473.

[73] H. Joshi, O. Prakash, A.K. Sharma, K.N. Sharma, A.K. Singh, Suzuki coupling reactions catalyzed with palladacycles and palladium(II) complexes of 2-thiophenemethylamine-based Schiff bases: examples of divergent pathways for the same ligand: Suzuki coupling reactions, 2015, Eur. J. Inorg. Chem. (2015) 1542–1551, https://doi.org/10.1002/ejic.201403176.

[74] S. Kumar, G.K. Rao, A. Kumar, M.P. Singh, F. Saleem, A.K. Singh, Efficient catalytic activation of Suzuki–Miyaura C–C coupling reactions with recyclable palladium nanoparticles tailored with sterically demanding di-n-alkyl sulfides, RSC Adv. 5 (2015) 20081–20089, https://doi.org/10.1039/c5ra00441a.

[75] E. Mohammadi, B. Movassagh, Polystyrene-resin supported N-heterocyclic carbene-Pd(II) complex based on plant-derived theophylline: a reusable and effective catalyst for the Suzuki-Miyaura cross-coupling reaction of arenediazonium tetrafluoroborate salts with arylboronic acids, J. Organomet. Chem. 822 (2016) 62–66, https://doi.org/10.1016/j.jorganchem.2016.08.017.

[76] M. Akkoç, N. Buğday, S. Altın, N. Kiraz, S. Yaşar, İ. Özdemir, N-heterocyclic carbene Pd(II) complex supported on $Fe_3O_4@SiO_2$: highly active, reusable and magnetically separable catalyst for Suzuki-Miyaura cross-coupling reactions in aqueous media, J. Organomet. Chem. 943 (2021), 121823, https://doi.org/10.1016/j.jorganchem.2021.121823.